



Review

Developments in FTICR-MS and Its Potential for Body Fluid Signatures

Simone Nicolardi ¹, Bogdan Bogdanov ², André M. Deelder ¹, Magnus Palmblad ¹ and Yuri E. M. van der Burgt ^{1,*}

Received: 22 September 2015 ; Accepted: 5 November 2015 ; Published: 13 November 2015

Academic Editor: Laszlo Prokai

¹ Center for Proteomics and Metabolomics, Leiden University Medical Center (LUMC), PO Box 9600, 2300 RC Leiden, The Netherlands; s.nicolardi@lumc.nl (S.N.); a.m.deelder@lumc.nl (A.M.D.); n.m.palmblad@lumc.nl (M.P.)

² PerkinElmer, San Jose Technology Center, San Jose, CA 95134, USA; bogdan.bogdanov@perkinelmer.com

* Correspondence: y.e.m.van_der_burgt@lumc.nl; Tel.: +31-71-526-9527

Abstract: Fourier transform mass spectrometry (FTMS) is the method of choice for measurements that require ultra-high resolution. The establishment of Fourier transform ion cyclotron resonance (FTICR) MS, the availability of biomolecular ionization techniques and the introduction of the Orbitrap™ mass spectrometer have widened the number of FTMS-applications enormously. One recent example involves clinical proteomics using FTICR-MS to discover and validate protein biomarker signatures in body fluids such as serum or plasma. These biological samples are highly complex in terms of the type and number of components, their concentration range, and the structural identity of each species, and thus require extensive sample cleanup and chromatographic separation procedures. Clearly, such an elaborate and multi-step sample preparation process hampers high-throughput analysis of large clinical cohorts. A final MS read-out at ultra-high resolution enables the analysis of a more complex sample and can thus simplify upfront fractionations. To this end, FTICR-MS offers superior ultra-high resolving power with accurate and precise mass-to-charge ratio (m/z) measurement of a high number of peptides and small proteins (up to 20 kDa) at isotopic resolution over a wide mass range, and furthermore includes a wide variety of fragmentation strategies to characterize protein sequence and structure, including post-translational modifications (PTMs). In our laboratory, we have successfully applied FTICR “next-generation” peptide profiles with the purpose of cancer disease classifications. Here we will review a number of developments and innovations in FTICR-MS that have resulted in robust and routine procedures aiming for ultra-high resolution signatures of clinical samples, exemplified with state-of-the-art examples for serum and saliva.

Keywords: mass spectrometry; proteomics; solid-phase extraction; ultra-high resolving power; FTICR-MS; instrumental development; serum; saliva; clinical cohort; profiling

1. Introduction

Fourier transform ion cyclotron resonance (FTICR) mass spectrometry (MS) offers the highest resolving power, resolution, and mass-to-charge ratio (m/z) measurement accuracy of all existing MS techniques [1]. This unparalleled performance has been heavily challenged since the commercial introduction of the Orbitrap™ mass spectrometer, the newest member of the FTMS family [2]. Nevertheless, the Orbitrap’s inventor himself stated that “inherent stability and field uniformity of superconducting magnets in synergy with the very high accuracy and dynamic range of frequency measurements made this technique an ultimate champion in mass resolving power and mass accuracy” [3]. The isotopic distribution accuracy, a wide intra- and inter-spectrum dynamic

range, and high sensitivity all make FTICR-MS the technique of choice to analyze samples of high complexity and identify thousands of compounds simultaneously with high confidence, with petroleomics and analysis of complex natural products being key examples [4–6]. In addition, FTICR plays its role in bottom-up and top-down proteomics approaches, and recently also in middle-down applications [7–9]. Since its introduction forty years ago the basic design has not changed: internally or externally generated ions are radially trapped in a strong magnetic field combined with a weak axial electric field, the image current is being detected from the coherently excited trapped ions, and the resulting time-domain signal is digitized and converted using Fourier transform (FT) into the frequency-domain spectrum and finally into a mass spectrum [10]. In addition, FTICR-MS has undergone many technological improvements of its various components, both with regard to hardware and software. Improved resolving power, resolution, m/z -accuracy, dynamic range, and sensitivity of FTICR-MS are not the result of the development of a single instrument component. Modern FTICR instruments are truly wonders of science and engineering. For the main portion of its lifetime FTICR-MS has been the domain of the academic research environment, but nowadays commercial instruments are available to a larger and less specialized group of users, mainly because of the development of easy-to-use control software which required less or no instrument tuning and the possibility to set up complex experiments. This development has also opened the door towards large-scale clinical applications. Here we will overview these instrumental improvements and present two different examples of body fluid signatures obtained with FTICR-MS, namely peptides and small proteins from serum and peptides from saliva.

2. FTICR-MS Instrumental Developments

2.1. FTICR-MS Components

Most FTICR-MS applications are based on electrospray ionization (ESI) or other atmospheric pressure ionization techniques to generate and introduce ions into the instrument [11]. Studies that use matrix-assisted laser desorption/ionization (MALDI) have been reported less frequently despite the excellent fit of MALDI and FTICR-MS [12–16]. In both cases ions enter the instrument after generation at atmospheric pressure and make their way towards the ultra-high vacuum (UHV) region and into the ICR cell that resides inside the homogeneous region of a high-field superconducting magnet. Improved inlet capillaries and the use of the ion funnel have reduced the ion losses dramatically by making the first stage of the ion transfer more efficient [17]. New ion funnel designs like the dual ion funnel, the high-pressure ion funnel, and the ion funnel trap have been or will be able to improve FTICR-MS even more when implemented [18–20]. Implementation of the RF/DC selection quadrupole and the linear ion trap have contributed to the increase in the dynamic range, in addition to providing more selective tandem mass spectrometry (MS/MS) capabilities [21,22]. The dynamic range enhancement applied to mass spectrometry (DREAMS) technology developed at the Pacific Northwest National Laboratory (PNNL) by Smith and co-workers improves the detectability of lower ion count peptides among high ion count co-eluting peptides, but unfortunately never has been commercialized even though it was implemented on an LTQ-FT instrument with automatic gain control (AGC) capabilities [23]. After ion trapping in a multipole ion guide/trap, the ions have to be ejected towards the ICR cell for the second trapping event and angled extraction wires have made this process more efficient [24]. Even though a field-free flight tube has been implemented, the use of a multipole ion guide offers a more efficient option to accomplish the ion transfer to the ICR cell. However, time-of-flight effects during the ion transfer might lead to skewed mass spectrum appearances [25]. In order to reduce these effects, solutions like the restrained ion population transfer, a shorter ion guide, multiple ion filling and transfer times, and the hexapole and octopole ion guides have been implemented [25–28]. In addition, various effects when the ions enter the magnetic field have been reported and accounted for [29,30]. Finally, advances in data acquisition, storage, processing, and analysis have been detrimental. Calibration taking into account

ion population dependency, the “walking” calibration, and artificial neural network calibration have made sub-ppb mass accuracy possible [31–33]. In addition, centroid data storage, absorption mode/phase correction, apodization/zero-filling, double/multiple frequency measurements, and perhaps in the future the filter diagonalization method (FDM) or other alternatives instead of FT have or will make FTICR faster and perform better [34–37].

2.2. ICR Cell Ion Trapping and MS/MS

Initially, gas-assisted ion trapping was needed during the ICR cell ion trapping event. This prevented high-throughput applications of FTICR-MS because of the low-duty cycle due to the time required to remove trapping gas to obtain UHV essential for improved FTICR-MS performance. After the implementation of an extra external trapping event new ICR trapping methods like side-kick and gated trapping were introduced and the gas pulse was no longer needed [38–40]. FTICR-MS performance is very sensitive to the ion population inside the ICR cell [41]. Too many ions in the ICR cell will lead to space charge effects and frequency shifts might occur, which could influence the resolving power, the dynamic range, the m/z -accuracy, and the peak shapes [42]. The introduction of AGC, which was commonly used for the same reasons on quadrupole ion trap instruments, for FTICR-MS was a big step towards tackling these challenges [22]. Once inside, the ICR cell the ions can undergo various events like an additional high resolution ion isolation, for both single or multiple ions by CHEF or SWIFT or the multiplexed analogues, respectively, ion-molecule reactions like HDX, or MS/MS by sustained off-resonance irradiation—collision-induced dissociation (SORI-CID), electron capture dissociation (ECD), infrared multi-photon dissociation (IRMPD), ultraviolet photo-dissociation (UVPD), or surface-induced dissociation (SID) [43–50]. Ion excitation has been performed by applying CHIRP or SWIFT waveforms and the excitation radius has a noticeable influence on the FTICR merits of performance [51–53]. In addition, the transient lifetime could be extended by applying electron promoted ion coherence (EPIC), and 60° excitation plates (and consequently 120° detection plates) showed the expected improved performance [25,54]. Improved designs of the pre-amplifier and the ICR cell UHV by using turbo pumps with magnetic field shielding have made their positive contributions as well [55,56].

2.3. ICR Cell Improvements

The increase in the magnetic field strength (B) and its homogeneity has been very important to the performance improvements. Until very recently, the highest magnetic field strength with a superconducting wide bore magnet was 15 tesla. Since then, two FTICR-MS systems equipped with 21 tesla superconducting magnets have been installed at the National High Magnetic Field Laboratory (NHMFL) and at PNNL [57,58]. The increase in the magnetic field strength improves the resolving power, the highest non-coalesced mass, the duty cycle (all proportional to B), and the trapped-ion upper mass, the ion trapping time, the ion energy, and the number ions (all proportional to B^2) [59]. The first publicly shared results of the NHMFL 21 tesla FTICR showed the expected and impressive results [57]. The ICR cell is the other key element that has attracted a lot of attention to improve upon and over the past forty years many different designs have been developed [59]. The original cubic ICR cell has been succeeded by mainly cylindrical-shaped designs, although a hyperbolic design has been reported [60,61]. Only the matrix-shimmed cube design was a reminder of how it all once started [62]. The cylindrical designs are either open (with four trapping plates on each side of the two excitation and detection plates, and either uncoupled or coupled trapping and excitation plates), or closed (with two cylindrical trapping plates in the xy plane) [63,64]. The “infinity” cell is a version of the closed cylindrical ICR cell [39]. In addition, various dual-cell designs have been reported [65,66]. Over the past decade a relatively large number of innovative ICR cells have been designed and constructed and the main goal of all designs was to increase the resolving power by extending the transient lifetime and to decrease the space-charge effects and resulting frequency shifts to maintain a high m/z -measurement accuracy without compromising peak shapes

through peak splitting or peak coalescence. For more detailed descriptions and motivations, we refer the reader to the cited references [57–66]. The complexity of the ion motion inside an ICR cell and the interactions of the three motion components, the cyclotron rotation, the trapping oscillation, and the magnetron rotation, all with their own m/z -dependent frequency, have led to various approaches and resulting ICR cell designs [59]. The trapping ring electrode cell, the electrically compensated cell, the grid/Ultra cell, the multipole cell, the open cylindrical seven segment cell [67], the temperature-controlled cell, the coaxial multi-electrode cell/O-trap, the dynamically harmonized cell, and the narrow aperture detection electrodes cell all have shown the targeted improvements on the FTICR-MS performance [53,67–74]. One of the most recent additions, the dynamically harmonized cell, has been extensively characterized theoretically and several new resolving power records have been accomplished [41,75,76]. Initially, using a 7 tesla FTICR-MS instrument for protonated reserpine a resolving power of 24,000,000 was obtained using a 180 s time domain signal, and for the 49+ charge state of bovine serum albumin (BSA) a resolving power of 1,200,000 was obtained [73]. Next, using a different 7 tesla FTICR-MS instrument and applying phase correction (the absorption-mode) for protonated reserpine, a resolving power of 32,000,000 was obtained [77]. Minor frequency shifts were observed when changing the excitation radius and accurate isotope fine structure was determined for the peak distributions of reserpine and Substance P, hereby confirming the elemental compositions [78]. In addition, the dynamically harmonized cell is commercially available on the Bruker Daltonics Solarix XR™ FTICR (Bremen, Germany) instrument so a larger audience can have access to ultra-high resolution MS capabilities and their benefits to solve scientific questions that other MS technologies cannot [79].

3. State-of-the-Art FTICR-MS Body Fluid Peptide and Protein Signatures

In this part of the review we present two examples of body fluid signatures obtained on a 15 tesla FTICR-MS instrument equipped with an ESI/MALDI ion source and an implemented dynamically harmonized cell. For most practical proteomics and metabolomics ESI-based applications resolving powers of 100,000–200,000 are sufficient, which are values that can only be obtained by FTICR and Orbitrap™ instruments and currently not by any commercially available TOF instrument. Previously, we have reported various high-throughput solutions for balancing the speed of the current FTICR-MS-acquisitions (“measurements”) and the time needed for analytical cleanup of body fluids (“sample preparation”) [13,80–82]. In this context it is stressed that time-consuming sample preparation procedures such long-gradient bottom-up liquid chromatography (LC)-MS/MS proteomics workflows are impracticable for high-throughput analyses. Moreover, such approaches require specific optimization to allow a robust and reproducible throughput of complex biological samples. A robotic pipetting platform for single-step sample cleanup and separation of complex protein mixtures is extremely helpful in providing a high degree of standardization. With proper calibration and maintenance of the liquid handling system on a regular basis, all procedures are performed in exactly the same way and as a result the precision improves of the sample preparation is improved [82–84]. Furthermore, sample processing times can be decreased and automation enables 24/7 performance.

3.1. Example 1: MALDI-FTICR-MS Profiling of Serum Peptides and Proteins

Proteins and peptides were isolated (fractionated) from human serum samples using functionalized paramagnetic beads purchased from Invitrogen (reversed-phase (RP) C18 Dynabeads; Carlsbad, CA, USA) as described previously [80,85]. Briefly, a single-step serum cleanup procedure based on solid-phase extraction (SPE) was combined with MALDI-FTICR readout. Fresh RPC18-functionalized magnetic beads were first activated by a three-step washing protocol on a fully automated 96-channel liquid handling system. Then, the serum samples were added and incubated, followed by washing the beads and eluting the peptides with a 1:1 mixture of water and acetonitrile. Spotting onto a MALDI AnchorChip™ (Bruker Daltonics, Bremen,

Germany) target plate was performed in combination with a mixing protocol using MALDI matrix α -cyano-4-hydroxycinnamic acid (CHCA, Bruker Daltonics, Bremen, Germany). MALDI-FTICR profiles were obtained on a Bruker 15 tesla Solarix XR™ FTICR mass spectrometer equipped with an ESI/MALDI CombiSource™, a novel ParaCell™ and a Bruker Smartbeam-II™ Laser System. Two acquisition settings (a low-mass (LM) and high-mass (HM) method) were used to optimize both the sensitivity and the resolving power in the range from 1012 to 5000 m/z -units and from 3497 to 30,000 m/z -units, respectively. A typical example of a compiled MALDI-FTICR “RPC18-profile” of a human serum sample is presented in Figure 1. For comparison, a MALDI-time-of-flight (TOF) profile of the same sample is shown in combination with this ultra-high resolution profile. MALDI-TOF is by far the most widely used strategy in MS-based biomarker profiling studies [86–91]. Unfortunately, amongst other issues, the identification of discriminating features (*i.e.*, peptides) in such MALDI-TOF profiles has been rather unsuccessful. Here, two beneficial aspects of ultra-high resolution of FTICR come into play: all species observed in Figure 1 were isotopically resolved up to 19,000 mass units thus facilitating their identification, and overlapping signals can be resolved. Furthermore, it follows from Figure 1 that the relative intensities of all species do not simply overlay between TOF and FTICR. This illustrates that the signatures are platform-specific and stresses the need for calibrators for quantification purposes [83].

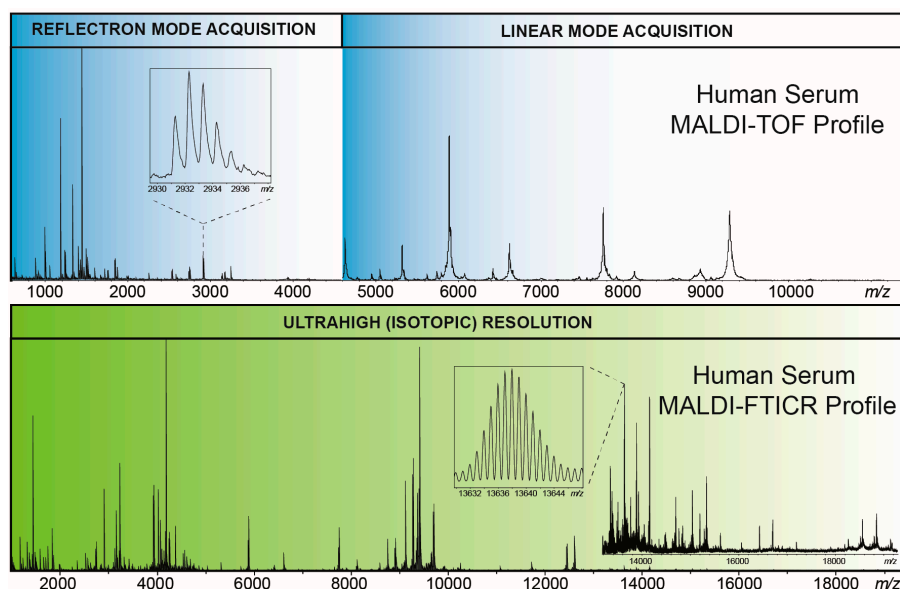


Figure 1. Early (in blue) and current (in green) matrix-assisted laser desorption/ionization (MALDI)-based serum peptide and protein profiles obtained after reversed-phase (RP) C18-magnetic bead cleanup. The MALDI-time-of-flight (TOF) profile in the upper panel is composed of a low-resolution linear mode spectrum (up to m/z -value 11,000) and a high-resolution reflectron mode spectrum (up to m/z -value 4600); in the lower panel a MALDI- Fourier transform ion cyclotron resonance (FTICR) profile of the same sample is shown.

3.2. Example 2: MALDI-FTICR-MS Profiling of Salivary Peptides and Proteins

As a second example a typical MALDI-FTICR “RPC18-profile” of a human saliva sample is presented in Figure 2. Note that all species observed in Figure 2 were isotopically resolved up to 15,000 mass units. The ultra-high resolution of FTICR enables structure characterizations of (interesting) features in a profile. This is even more facilitated in the ESI-mode when on the same system a profile is obtained with multiply charged species. These are convenient for identification purposes, as is demonstrated at the bottom of Figure 2. Two large peptides were identified from a CID- and an ETD-MS/MS spectrum, respectively.

Provided the MALDI-based profiles can be obtained in a robust way, that is, at minimum considering the basic analytical quality requirements, these peptide and protein signatures have potential for clinical applications [83]. Topics such as costs of the MS-system and “return-on-investment” obviously become important when aiming for future routine measurements and implementation as an assay. Clearly, FTICR platforms are expensive and operating costs are higher than for an Orbitrap™ system due to the need for liquid helium. However, FTICR magnets last long (more than 15 years is not uncommon) and instrument down-time is low. Consequently, it may well be that the comparison with other routine, often also expensive clinical assays is beneficial for FTICR. Furthermore, FTICR data storage is no longer a limiting factor and current systems allow future re-analysis, which is advantageous for longitudinal studies.

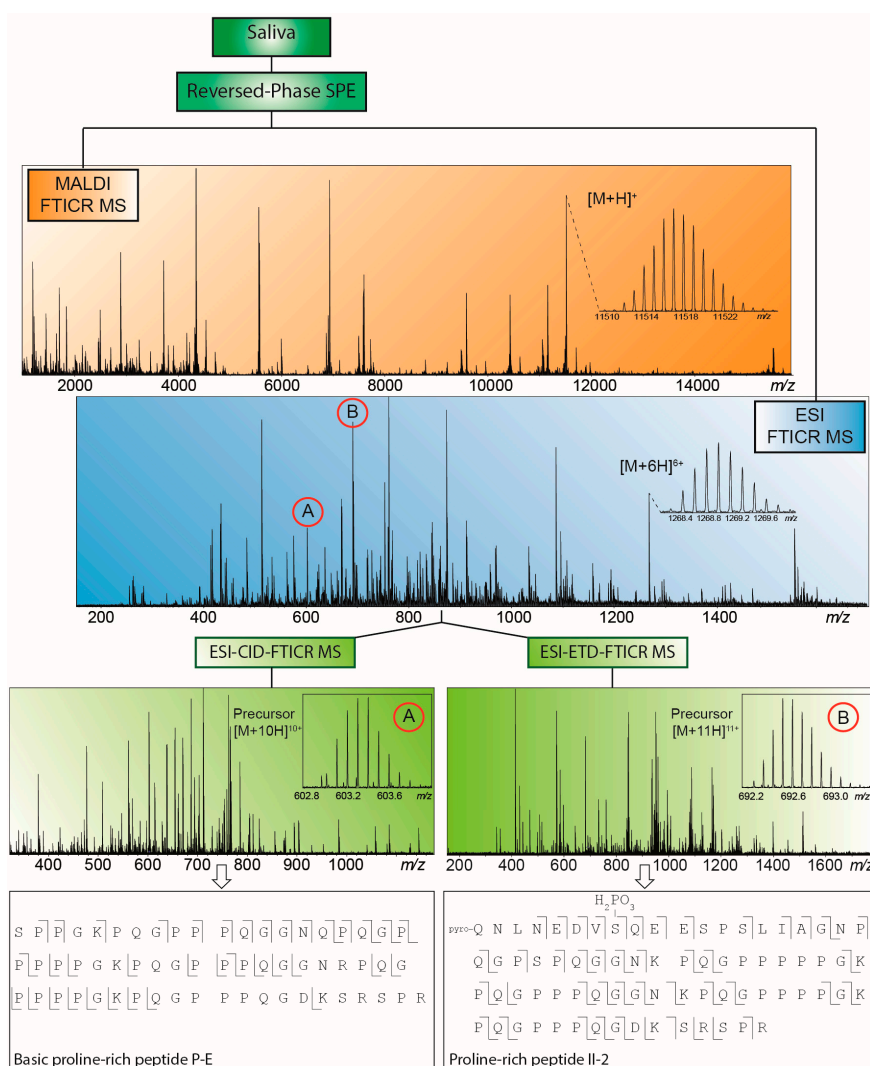


Figure 2. MALDI-FTICR (in orange) and electrospray ionization (ESI)-FTICR (in blue) saliva peptide and protein profiles obtained after RPC18-based cleanup. Multiply charged species in the ESI-FTICR profile (indicated with A and B) were selected for tandem mass spectrometry (MS/MS) analysis, with identification results shown at the bottom (in green).

4. Conclusions and Future Outlook

The most recent promising improvements in FTICR hardware and software have been made at universities and national labs. With only one FTICR manufacturer left and the reality of patents and licenses, it might be some time before some of these will be available on commercial instruments.

However, the current FTICR instruments have many more advanced technologies compared to a decade ago and are suitable for the kind of high throughput clinical screening applications described here. As was shown in this review, peptide and protein signatures can be obtained via a standardized and automated one-step sample cleanup strategy in combination with high-end MS readout using ultra-high resolution equipment. These signatures can be classified and provide a solid platform for rapid screening of body fluids in order to further select a sub-set for detailed (or in-depth) analysis. These workflows can also be applied for the analysis of lipids, and glycans and glycopeptides derived from glycoproteins [84]. Hyphenation of ion mobility, using either high-field asymmetric waveform ion mobility mass spectrometry (FAIMS) or drift tubes, and FTICR will open new opportunities to increase the dynamic range and the selectivity. It will be interesting to see if the m/z -range of FTICR can be further extended (to for instance m/z -values of 25,000 or even up to 50,000) so more proteins can be detected and to follow developments in Orbitrap™ technology. This will not only be of interest for MALDI-based profiling studies, but also for tissue-based MALDI-MS imaging research [92,93]. It is further noted that the application of direct infusion native nano-ESI in (clinical) protein screening or analysis of biopharmaceuticals might gain interest. For example, protein complexes and viruses have been analyzed on an optimized Orbitrap™ platform [94,95]. Finally, sub-ppm mass precision and accuracy allow determination of isotopic distributions and exact mass measurements and open the way for isotopic fine structure analyses for identification purposes [78,96].

Author Contributions: Bogdan Bogdanov, André M. Deelder and Yuri E. M. van der Burgt initiated the idea of writing this review together. Bogdan Bogdanov, Simone Nicolardi and Yuri E. M. van der Burgt wrote Parts 1 and 2. Simone Nicolardi performed the experiments and data analysis shown in Figures 1 and 2 and Yuri E. M. van der Burgt supervised this work (Part 3). Writing of the manuscript was furthermore performed by André M. Deelder and Magnus Palmblad.

Conflicts of Interest: The authors declare no conflict of interest.

References

1. Marshall, A.G. Milestones in Fourier transform ion cyclotron resonance mass spectrometry technique development. *Int. J. Mass Spectrom.* **2000**, *200*, 331–356. [[CrossRef](#)]
2. Makarov, A. Electrostatic axially harmonic orbital trapping: A high-performance technique of mass analysis. *Anal. Chem.* **2000**, *72*, 1156–1162. [[CrossRef](#)] [[PubMed](#)]
3. Zubarev, R.A.; Makarov, A.A. Orbitrap mass spectrometry. *Anal. Chem.* **2013**, *85*, 5288–5296. [[CrossRef](#)] [[PubMed](#)]
4. Hughey, C.A.; Rodgers, R.P.; Marshall, A.G. Resolution of 11000 compositionally distinct components in a single electrospray ionization Fourier transform ion cyclotron resonance mass spectrum of crude oil. *Anal. Chem.* **2002**, *74*, 4145–4149. [[CrossRef](#)] [[PubMed](#)]
5. Marshall, A.G.; Rodgers, R.P. Petroleomics: Chemistry of the underworld. *Proc. Natl. Acad. Sci. USA* **2008**, *105*, 18090–18095. [[CrossRef](#)] [[PubMed](#)]
6. Cho, Y.; Ahmed, A.; Islam, A.; Kim, S. Developments in FT-ICR instrumentation, ionization techniques, and data interpretation methods for petroleomics. *Mass Spectrom. Rev.* **2015**, *34*, 248–263. [[CrossRef](#)] [[PubMed](#)]
7. Bogdanov, B.; Smith, R.D. Proteomics by FTICR mass spectrometry: Top down and bottom up. *Mass Spectrom. Rev.* **2005**, *24*, 168–200. [[CrossRef](#)] [[PubMed](#)]
8. Johansson, Å.; Enroth, S.; Palmblad, M.; Deelder, A.M.; Bergquist, J.; Gyllenstein, U. Identification of genetic variants influencing the human plasma proteome. *Proc. Natl. Acad. Sci. USA* **2013**, *110*, 4673–4378.
9. Kalli, A.; Sweredoski, M.J.; Hess, S. Data-dependent middle-down nano-liquid chromatography-electron capture dissociation-tandem mass spectrometry: An application for the analysis of unfractionated histones. *Anal. Chem.* **2013**, *85*, 3501–3507. [[CrossRef](#)] [[PubMed](#)]
10. Comisarow, M.B.; Marshall, A.G. Fourier transform ion cyclotron resonance spectroscopy. *Chem. Phys. Lett.* **1974**, *25*, 282–283. [[CrossRef](#)]
11. Fenn, J.B.; Mann, M.; Meng, C.K.; Wong, S.F.; Whitehouse, C.M. Electrospray ionization for mass spectrometry of large biomolecules. *Science* **1989**, *246*, 64–71. [[CrossRef](#)] [[PubMed](#)]

12. Karas, M.; Bachmann, D.; Hillenkamp, F. Influence of the wavelength in high-irradiance ultraviolet laser desorption mass spectrometry of organic molecules. *Anal. Chem.* **1985**, *57*, 2935–2939. [[CrossRef](#)]
13. Cancilla, M.T.; Penn, S.G.; Carroll, J.A.; Lebrilla, C.B. Coordination of alkali metals to oligosaccharides dictates fragmentation behavior in matrix assisted laser desorption ionization Fourier transform mass spectrometry. *J. Am. Chem. Soc.* **1996**, *118*, 6736–6745. [[CrossRef](#)]
14. Nicolardi, S.; Palmblad, M.; Hensbergen, P.J.; Tollenaar, R.A.E.M.; Deelder, A.M.; van der Burgt, Y.E.M. Precision profiling and identification of human serum peptides using Fourier transform ion cyclotron resonance mass spectrometry. *Rapid Commun. Mass Spectrom.* **2011**, *25*, 3457–3463. [[CrossRef](#)] [[PubMed](#)]
15. Nicolardi, S.; van der Burgt, Y.E.M.; Wuhrer, M.; Deelder, A.M. Mapping O-glycosylation of apolipoprotein C-III in MALDI-FT-ICR protein profiles. *Proteomics* **2013**, *13*, 992–1001. [[CrossRef](#)] [[PubMed](#)]
16. Nicolardi, S.; Switzar, L.; Deelder, A.M.; Palmblad, M.; van der Burgt, Y.E.M. Top-down MALDI-in-source decay-FTICR mass spectrometry of isotopically resolved proteins. *Anal. Chem.* **2015**, *87*, 3429–3437. [[CrossRef](#)] [[PubMed](#)]
17. Shaffer, S.A.; Tang, K.; Anderson, G.A.; Prior, D.C.; Udseth, H.R.; Smith, R.D. A novel ion funnel for focusing ions at elevated pressure using electrospray ionization mass spectrometry. *Rapid Commun. Mass Spectrom.* **1997**, *11*, 1813–1817. [[CrossRef](#)]
18. Hossain, M.; Kaleta, D.T.; Robinson, E.W.; Liu, T.; Zhao, R.; Page, J.S.; Kelly, R.T.; Moore, R.J.; Tang, K.; Camp, D.G., II; *et al.* Enhanced sensitivity for selected reaction monitoring mass spectrometry-based targeted proteomics using a dual stage electrodynamic ion funnel interface. *Mol. Cell. Proteom.* **2011**, *10*. [[CrossRef](#)] [[PubMed](#)]
19. Ibrahim, Y.; Tang, K.; Tolmachev, A.V.; Shvartsburg, A.A.; Smith, R.D. Improving mass spectrometer sensitivity using a high-pressure electrodynamic ion funnel interface. *J. Am. Soc. Mass Spectrom.* **2006**, *17*, 1299–1305. [[CrossRef](#)] [[PubMed](#)]
20. Ibrahim, Y.; Belov, M.E.; Tolmachev, A.V.; Prior, D.C.; Smith, R.D. Ion funnel trap interface for orthogonal time-of-flight mass spectrometry. *Anal. Chem.* **2007**, *79*, 7845–7852. [[CrossRef](#)] [[PubMed](#)]
21. Harkewicz, R.; Belov, M.E.; Anderson, G.A.; Paša-Tolić, L.; Masselon, C.D.; Prior, D.C.; Udseth, H.R.; Smith, R.D. ESI-FTICR Mass spectrometry employing data-dependent external ion selection and accumulation. *J. Am. Soc. Mass Spectrom.* **2002**, *13*, 144–154. [[CrossRef](#)]
22. Syka, J.E.; Marto, J.A.; Bai, D.L.; Horning, S.; Senko, M.W.; Schwartz, J.C.; Ueberheide, B.; Garcia, B.; Busby, S.; Muratore, T.; *et al.* Novel linear quadrupole ion trap/FT mass spectrometer: Performance characterization and use in the comparative analysis of histone H3 post-translational modifications. *J. Prot. Res.* **2004**, *3*, 621–626. [[CrossRef](#)]
23. Belov, M.E.; Anderson, G.A.; Angell, N.H.; Shen, Y.; Tolić, N.; Udseth, H.R.; Smith, R.D. Dynamic range expansion applied to mass spectrometry based on data-dependent selective ion ejection in capillary liquid chromatography Fourier transform ion cyclotron resonance for enhanced proteome characterization. *Anal. Chem.* **2001**, *73*, 5052–5060. [[CrossRef](#)] [[PubMed](#)]
24. Wilcox, B.E.; Hendrickson, C.L.; Marshall, A.G. Improved ion extraction from a linear octopole ion trap: SIMION analysis and experimental demonstration. *J. Am. Soc. Mass Spectrom.* **2002**, *13*, 1304–1312. [[CrossRef](#)]
25. Kaiser, N.K.; Quinn, J.P.; Blakney, G.T.; Hendrickson, C.L.; Marshall, A.G. A Novel 9.4 Tesla FTICR mass spectrometer with improved sensitivity, mass resolution, and mass range. *J. Am. Soc. Mass Spectrom.* **2011**, *22*, 1343–1351. [[CrossRef](#)] [[PubMed](#)]
26. Kaiser, N.K.; Skulason, G.E.; Weisbrod, C.R.; Wu, S.; Zhang, K.; Prior, D.C.; Buschbach, M.A.; Anderson, G.A.; Bruce, J.E. Restrained ion population transfer: A novel ion transfer method for mass spectrometry. *Rapid Commun. Mass Spectrom.* **2008**, *22*, 1955–1964. [[CrossRef](#)] [[PubMed](#)]
27. Chan, T.-W.D.; Duan, L.; Sze, T.-P.E. Accurate mass measurements for peptide and protein mixtures by using matrix-assisted laser desorption/ionization Fourier transform mass spectrometry. *Anal. Chem.* **2002**, *74*, 5282–5289. [[CrossRef](#)] [[PubMed](#)]
28. McIver, R.T.; Hunter, R.L.; Bowers, W.D. Coupling a quadrupole mass spectrometer and a Fourier transform mass spectrometer. *Int. J. Mass Spectrom. Ion Proc.* **1985**, *64*, 67–77. [[CrossRef](#)]
29. McIver, R.T. Trajectory calculations for axial injection of ions into a magnetic field: Overcoming the magnetic mirror effect with an rf quadrupole lens. *Int. J. Mass Spectrom. Ion Proc.* **1990**, *98*, 35–50. [[CrossRef](#)]

30. Beu, S.C.; Hendrickson, C.L.; Marshall, A.G. Excitation of radial ion motion in an rf-only multipole ion guide immersed in a strong magnetic field gradient. *J. Am. Soc. Mass Spectrom.* **2011**, *22*, 591–601. [[CrossRef](#)] [[PubMed](#)]
31. Williams, D.K.; Muddiman, D.C. Parts-per-billion mass measurement accuracy achieved through the combination of multiple linear regression and automatic gain control in a Fourier transform ion cyclotron resonance mass spectrometer. *Anal. Chem.* **2007**, *79*, 5058–5063. [[CrossRef](#)] [[PubMed](#)]
32. Savory, J.J.; Kaiser, N.K.; McKenna, A.M.; Xian, F.; Blakney, G.T.; Rodgers, R.P.; Hendrickson, C.L.; Marshall, A.G. Parts-per-billion Fourier transform ion cyclotron resonance mass measurement accuracy with a “walking” calibration equation. *Anal. Chem.* **2011**, *83*, 1732–1736. [[CrossRef](#)] [[PubMed](#)]
33. Williams, D.K.; Kovach, A.L.; Muddiman, D.C.; Hanck, K.W. Utilizing artificial neural networks in MATLAB to achieve parts-per-billion mass measurement accuracy with a Fourier transform ion cyclotron resonance mass spectrometer. *J. Am. Soc. Mass Spectrom.* **2009**, *20*, 1303–1310. [[CrossRef](#)] [[PubMed](#)]
34. Xian, F.; Hendrickson, C.L.; Blakney, G.T.; Beu, S.C.; Marshall, A.G. Automated broadband phase correction of Fourier transform ion cyclotron resonance mass spectra. *Anal. Chem.* **2010**, *82*, 8807–8812. [[CrossRef](#)] [[PubMed](#)]
35. Qian, Y.; O’Connor, P.B. Data processing in Fourier transform ion cyclotron resonance mass spectrometry. *Mass Spectrom. Rev.* **2014**, *33*, 333–352.
36. Kilgour, D.P.A.; Wills, R.; Qi, Y.; O’Connor, P.B. Autophaser: An algorithm for automated generation of absorption mode spectra for FT-ICR MS. *Anal. Chem.* **2013**, *85*, 3903–3911. [[CrossRef](#)] [[PubMed](#)]
37. Nagornov, K.O.; Gorshkov, M.V.; Kozhinov, A.N.; Tsybin, Y.O. High-resolution Fourier transform ion cyclotron resonance mass spectrometry with increased throughput for biomolecular analysis. *Anal. Chem.* **2014**, *86*, 9020–9028. [[CrossRef](#)] [[PubMed](#)]
38. Senko, M.W.; Hendrickson, C.L.; Emmett, M.R.; Shi, S.D.-H.; Marshall, A.G. External accumulation of ions for enhanced electrospray ionization Fourier transform ion cyclotron resonance mass spectrometry. *J. Am. Soc. Mass Spectrom.* **1997**, *8*, 970–976. [[CrossRef](#)]
39. Caravatti, P.U.S. Method and Apparatus for the Accumulation of Ions in a Trap of an Ion Cyclotron Resonance Spectrometer, by Transferring the Kinetic Energy of the Motion Parallel to the Magnetic Field into Directions Perpendicular to the Magnetic Field. Patent 4,924,089, 8 May 1990.
40. Alford, J.M.; Williams, P.E.; Trevor, D.J.; Smalley, R.E. Metal cluster ion cyclotron resonance. Combining supersonic metal cluster beam technology with FT-ICR. *Int. J. Mass Spectrom. Ion Proc.* **1986**, *72*, 33–51. [[CrossRef](#)]
41. Nikolaev, E.N.; Kostyukevich, Y.I.; Vladimirov, G.N. Fourier transform ion cyclotron resonance (FT ICR) mass spectrometry: Theory and simulations. *Mass Spectrom. Rev.* **2014**. [[CrossRef](#)] [[PubMed](#)]
42. Nikolaev, E.N. Some notes about FT ICR mass spectrometry. *Int. J. Mass Spectrom.* **2015**, *377*, 421–431. [[CrossRef](#)]
43. De Koning, L.J.; Nibbering, N.M.M.; van Orden, S.L.; Laukien, F.H. Mass selection of ions in a Fourier transform ion cyclotron resonance trap using correlated harmonic excitation fields (CHEF). *Int. J. Mass Spectrom. Ion Proc.* **1997**, *165–166*, 209–219. [[CrossRef](#)]
44. Guan, S.; Burlingame, A.L. High mass selectivity for top-down proteomics by application of SWIFT technology. *J. Am. Soc. Mass Spectrom.* **2010**, *21*, 455–459. [[CrossRef](#)] [[PubMed](#)]
45. Freitas, M.A.; Hendrickson, C.L.; Emmett, M.R.; Marshall, A.G. Gas-phase bovine ubiquitin cation conformations resolved by gas-phase hydrogen/deuterium exchange rate and extend. *Int. J. Mass Spectrom.* **1999**, *185*, 565–575. [[CrossRef](#)]
46. Gauthier, J.W.; Trautman, T.R.; Jacoson, D.B. Sustained off-resonance irradiation for collision-activated dissociation involving Fourier transform mass spectrometry. Collision-activated dissociation technique that emulates infrared multiphoton dissociation. *Anal. Chim. Acta* **1991**, *246*, 211–225. [[CrossRef](#)]
47. Zubarev, R.A.; Kelleher, N.L.; McLafferty, F.W. Electron capture dissociation of multiply charge protein cations: A nonergodic process. *J. Am. Chem. Soc.* **1998**, *120*, 3265–3266. [[CrossRef](#)]
48. Little, D.P.; Speir, J.P.; Senko, M.W.; O’Connor, P.B.; McLafferty, F.W. Infrared multiphoton dissociation of large multiply charged ions for biomolecule sequencing. *Anal. Chem.* **1994**, *66*, 2809–2815. [[CrossRef](#)] [[PubMed](#)]
49. Bowers, W.D.; Delbert, S.S.; Hunter, R.L.; McIver, R.T. Fragmentation of oligopeptide ions using ultraviolet laser radiation and Fourier transform mass spectrometry. *J. Am. Chem. Soc.* **1984**, *106*, 7288–7289. [[CrossRef](#)]

50. Laskin, J.; Denisov, E.V.; Shukla, A.K.; Barlow, S.E.; Futrell, J.H. Surface-induced dissociation in a Fourier transform ion cyclotron resonance mass spectrometer: Instrument design and evaluation. *Anal. Chem.* **2002**, *74*, 3255–3261. [[CrossRef](#)] [[PubMed](#)]
51. Marshall, A.G.; Roe, D.C. Theory of Fourier transform ion cyclotron resonance mass spectroscopy: Response to frequency-sweep excitation. *J. Chem. Phys.* **1980**, *73*, 1581–1590. [[CrossRef](#)]
52. Guan, S.; Marshall, A.G. Stored waveform inverse Fourier transform (SWIFT) axial excitation/ejection for quadrupole ion trap mass spectrometry. *Anal. Chem.* **1993**, *65*, 1288–1294. [[CrossRef](#)] [[PubMed](#)]
53. Tolmachev, A.V.; Robinson, E.W.; Wu, S.; Kang, H.; Lourette, N.M.; Paša-Tolić, L.; Smith, R.D. Trapped-ion cell with improved DC potential harmonicity for FT-ICR MS. *J. Am. Soc. Mass Spectrom.* **2008**, *19*, 586–597. [[CrossRef](#)] [[PubMed](#)]
54. Kaiser, N.K.; Bruce, J.E. Reduction of ion magnetron motion and space charge using radial electric field modulation. *Int. J. Mass Spectrom.* **2007**, *265*, 271–280. [[CrossRef](#)]
55. Mathur, R.; Knepper, R.W.; O'Connor, P.B. A low-noise, wideband preamplifier for a Fourier-transform ion cyclotron resonance mass spectrometer. *J. Am. Soc. Mass Spectrom.* **2007**, *18*, 2233–2241. [[CrossRef](#)] [[PubMed](#)]
56. Kaiser, N.K.; Skulason, G.E.; Weisbrod, C.R.; Bruce, J.E. A novel Fourier transform ion cyclotron resonance mass spectrometer with improved ion trapping and detection capabilities. *J. Am. Soc. Mass Spectrom.* **2009**, *20*, 755–762. [[CrossRef](#)] [[PubMed](#)]
57. Hendrickson, C.L.; Quinn, J.P.; Kaiser, N.K.; Smith, D.F.; Blakney, G.T.; Chen, T.; Marshall, A.G.; Weisbrod, C.R.; Beu, S.C. 21 tesla Fourier transform ion cyclotron resonance mass spectrometer: A national resource for ultrahigh resolution mass analysis. *J. Am. Soc. Mass Spectrom.* **2015**, *26*, 1626–1632. [[CrossRef](#)] [[PubMed](#)]
58. BREAKING NEWS! EMSL's 21 T mass spectrometer at field. Available online: <http://www.emsl.pnl.gov/emslweb/news/breaking-news-emsl%E2%80%99s-21-t-mass-spectrometer-field> (accessed on 6 November 2015).
59. Marshall, A.G.; Hendrickson, C.L.; Jackson, G.S. Fourier transform ion cyclotron resonance mass spectrometry: A primer. *Mass Spectrom. Rev.* **1998**, *17*, 1–35. [[CrossRef](#)]
60. Comisarow, M.B.; Marshall, A.G. Fourier Transform Ion Cyclotron Resonance Spectroscopy Method and Apparatus. USA Patent No. 3,937,955, 14 February 1976.
61. Knight, R.D. The general form of the quadrupole ion trap potential. *Int. J. Mass Spectrom. Ion Proc.* **1983**, *51*, 515–518. [[CrossRef](#)]
62. Jackson, G.S.; White, F.M.; Guan, S.; Marshall, A.G. Matrix-shimmed ion cyclotron resonance ion trap simultaneously optimized for excitation, detection, quadrupolar axialization, and trapping. *J. Am. Soc. Mass Spectrom.* **1999**, *10*, 759–769. [[CrossRef](#)]
63. Beu, S.C.; Laude, D.A. Open trapped ion cell geometries for FT/ICR/MS. *Int. J. Mass Spectrom. Ion Proc.* **1992**, *112*, 215–230. [[CrossRef](#)]
64. Beu, S.C.; Laude, D.A. Elimination of axial ejection during excitation with a capacitively coupled open trapped cyclotron cell for Fourier transform ion cyclotron resonance mass spectrometry. *Anal. Chem.* **1992**, *64*, 177–180. [[CrossRef](#)]
65. Littlejohn, D.P.; Ghaderi, S. Mass spectrometer and method. USA Patent No. 4,581,533, 8 April 1986.
66. Gorshkov, M.V.; Paša-Tolić, L.; Bruce, J.E.; Anderson, G.A.; Smith, R.D. A dual-trap design and its applications in electrospray ionization FTICR mass spectrometry. *Anal. Chem.* **1997**, *69*, 1307–1314. [[CrossRef](#)] [[PubMed](#)]
67. Guoa, X.; Duursma, M.; Ahmed Al-Khalili, A.A.; McDonnell, L.A.; Heeren, R.M.A. Design and performance of a new FT-ICR cell operating at a temperature range of 77–438 K. *Int. J. Mass Spectrom.* **2004**, *231*, 37–45. [[CrossRef](#)]
68. Brustkern, A.M.; Rempel, D.L.; Gross, M.L. An electrically compensated trap designed to eighth order for FT-ICR mass spectrometry. *J. Am. Soc. Mass Spectrom.* **2008**, *19*, 1281–1285. [[CrossRef](#)] [[PubMed](#)]
69. Wieghaus, A.; Fröhlich, U.; Malek, R.; Horning, S. The grid cell: A new cell design for reduced z-axis ejection in fourier transform ion cyclotron mass spectrometry. In Proceedings of the 54th ASMS Conference on Mass Spectrometry and Allied Topics, Seattle, WA, USA, 28 May–1 June 2006.

70. Bruce, J.E.; Anderson, G.A.; Lin, C.-Y.; Gorshkov, M.; Rockwood, A.L.; Smith, R.D. A novel high-performance Fourier transform ion cyclotron resonance cell for improved biopolymer characterization. *J. Mass Spectrom.* **2000**, *35*, 85–94. [[CrossRef](#)]
71. Weisbrod, C.R.; Kaiser, N.K.; Skulason, G.E.; Bruce, J.E. Trapping ring electrode cell: A FTICR mass spectrometer cell for improved signal-to-noise and resolving power. *Anal. Chem.* **2008**, *80*, 6545–6553. [[CrossRef](#)] [[PubMed](#)]
72. Misharin, A.S.; Zubarev, R.A.; Doroshenko, V.M. Fourier transform ion cyclotron resonance mass spectrometer with coaxial multi-electrode cell (“O-trap”): First experimental demonstration. *Rapid Commun. Mass Spectrom.* **2010**, *24*, 1931–1940. [[CrossRef](#)] [[PubMed](#)]
73. Nikolaev, E.N.; Boldin, I.A.; Jertz, R.; Baykut, G. Initial experimental characterization of a new ultra-high resolution FTICR cell with dynamic harmonization. *J. Am. Soc. Mass Spectrom.* **2011**, *22*, 1125–1133. [[CrossRef](#)] [[PubMed](#)]
74. Nagornov, K.O.; Kozhinov, A.N.; Tsybin, O.Y.; Tsybin, Y.O. Ion trap with narrow aperture detection electrodes for Fourier transform ion cyclotron resonance mass spectrometry. *J. Am. Soc. Mass Spectrom.* **2015**, *26*, 741–751. [[CrossRef](#)] [[PubMed](#)]
75. Boldin, I.A.; Nikolaev, E.N. Fourier transform ion cyclotron resonance cell with dynamic harmonization of the electric field in the whole volume by shaping of the excitation and detection electrode assembly. *Rapid Commun. Mass Spectrom.* **2011**, *25*, 122–126. [[CrossRef](#)] [[PubMed](#)]
76. Kostyukevich, Y.I.; Vladimirov, G.N.; Nikolaev, E.N. Dynamically harmonized FT-ICR cell with specially shaped electrodes for compensation of inhomogeneity of the magnetic field. Computer simulations of the electric field and ion motion dynamics. *J. Am. Soc. Mass Spectrom.* **2012**, *23*, 2198–2207. [[CrossRef](#)] [[PubMed](#)]
77. Qi, Y.; Witt, M.; Jertz, R.; Baykut, G.; Barrow, M.P.; Nikolaev, E.N.; O’Connor, P.B. Absorption-mode spectra on the dynamically harmonized Fourier transform ion cyclotron resonance cell. *Rapid Commun. Mass Spectrom.* **2012**, *26*, 2021–2026. [[CrossRef](#)] [[PubMed](#)]
78. Nikolaev, E.N.; Jertz, R.; Grigoryev, A.; Baykut, G. Fine structure in isotopic peak distributions measured using a dynamically harmonized Fourier transform ion cyclotron resonance cell at 7 T. *Anal. Chem.* **2012**, *84*, 2275–2283. [[CrossRef](#)] [[PubMed](#)]
79. Bruker. Available online: <https://www.bruker.com/products/mass-spectrometry-and-separations/esimaldi-ftms/solarix/overview.html> (accessed on 9 November 2015).
80. Bladergroen, M.R.; Derks, R.J.; Nicolardi, S.; de Visser, B.; van Berloo, S.; van der Burgt, Y.E.M.; Deelder, A.M. Standardized and automated solid-phase extraction procedures for high-throughput proteomics of body fluids. *J. Proteom.* **2012**, *77*, 144–153. [[CrossRef](#)] [[PubMed](#)]
81. Nicolardi, S.; Velstra, B.; Mertens, B.J.; Bonsing, B.; Mesker, W.E.; Tollenaar, R.A.E.M.; Deelder, A.M.; van der Burgt, Y.E.M. Ultrahigh resolution profiles lead to more detailed serum peptidome signatures of pancreatic cancer. *Transl. Proteom.* **2014**, *2*, 39–51. [[CrossRef](#)]
82. Nicolardi, S.; Bladergroen, M.R.; Deelder, A.M.; Tollenaar, R.A.E.M.; Palmblad, M.; Mesker, W.E.; van der Burgt, Y.E.M. SPE-MALDI profiling of serum peptides and proteins by ultrahigh resolution FTICR-MS. *Chromatographia* **2015**, *78*, 445–449. [[CrossRef](#)]
83. Van den Broek, I.; Romijn, F.P.; Smit, N.P.; van der Laarse, A.; Drijfhout, J.W.; van der Burgt, Y.E.M.; Cobbaert, C.M. Quantifying protein measurands by peptide measurements: Where do errors arise? *J. Prot. Res.* **2015**, *14*, 928–942. [[CrossRef](#)] [[PubMed](#)]
84. Bladergroen, M.R.; Reiding, K.R.; Hipgrave Ederveen, A.L.; Vreeker, G.C.; Clerc, F.; Holst, S.; Bondt, A.; Wuhler, M.; van der Burgt, Y.E.M. Automation of high-throughput mass spectrometry-based plasma N-glycome analysis with linkage-specific sialic acid esterification. *J. Prot. Res.* **2015**, *14*, 1480–1486. [[CrossRef](#)] [[PubMed](#)]
85. Velstra, B.; Vonk, M.A.; Bonsing, B.; Mertens, B.J.; Nicolardi, S.; Huijbers, A.; Vasen, H.; Deelder, A.M.; Mesker, W.E.; van der Burgt, Y.E.M.; *et al.* Serum peptide signatures for pancreatic cancer based on mass spectrometry: A comparison to CA19–9 levels and routine imaging techniques. *J. Cancer Res. Clin. Oncol.* **2014**, *141*, 531–541. [[CrossRef](#)] [[PubMed](#)]
86. Marko-Varga, G.; Lindberg, H.; Löfdahl, C.G.; Jonsson, P.; Hansson, L.; Dahlback, M.; Lindquist, E.; Johansson, L.; Foster, M.; Fehniger, T.E. Discovery of biomarker candidates within disease by protein profiling: Principles and concepts. *J. Prot. Res.* **2005**, *4*, 1200–1212. [[CrossRef](#)] [[PubMed](#)]

87. Hortin, G.L. The MALDI-TOF mass spectrometric view of the plasma proteome and peptidome. *Clin. Chem.* **2006**, *52*, 1223–1237. [[CrossRef](#)] [[PubMed](#)]
88. Palmblad, M.; Tiss, A.; Cramer, R. Mass spectrometry in clinical proteomics—From the present to the future. *Proteom. Clin. Appl.* **2009**, *3*, 6–17. [[CrossRef](#)] [[PubMed](#)]
89. Magni, F.; van der Burgt, Y.E.M.; Chinello, C.; Mainini, V.; Gianazza, E.; Squeo, V.; Deelder, A.M.; Kienle, M.G. Biomarkers discovery by peptide and protein profiling in biological fluids based on functionalized magnetic beads purification and mass spectrometry. *Blood Transfus.* **2010**, *8*, 92–97.
90. Albrethsen, J. The first decade of MALDI protein profiling: A lesson in translational biomarker research. *J. Proteom.* **2011**, *74*, 765–773. [[CrossRef](#)] [[PubMed](#)]
91. Huijbers, A.; Mesker, W.E.; Mertens, B.J.; Bladergroen, M.R.; Deelder, A.M.; van der Burgt, Y.E.M.; Tollenaar, R.A.E.M. Case-controlled identification of colorectal cancer based on proteomic profiles and the potential for screening. *Colorectal Dis.* **2014**, *16*, 907–913. [[CrossRef](#)] [[PubMed](#)]
92. Taban, I.M.; Altelaar, A.F.; van der Burgt, Y.E.M.; McDonnell, L.A.; Heeren, R.M.; Fuchser, J.; Baykut, G. Imaging of peptides in the rat brain using MALDI-FTICR mass spectrometry. *J. Am. Soc. Mass Spectrom.* **2007**, *18*, 145–151. [[CrossRef](#)] [[PubMed](#)]
93. Spraggins, J.M.; Rizzo, D.G.; Moore, J.L.; Rose, K.L.; Hammer, N.D.; Skaar, E.P.; Caprioli, R.M. MALDI FTICR IMS of intact proteins: Using mass accuracy to link protein images with proteomics data. *J. Am. Soc. Mass Spectrom.* **2015**, *26*, 974–985. [[CrossRef](#)] [[PubMed](#)]
94. Belov, M.E.; Damoc, E.; Denisov, E.; Compton, P.D.; Horning, S.; Makarov, A.A.; Kelleher, N.L. From protein complexes to subunit backbone fragments: A multi-stage approach to native mass spectrometry. *Anal. Chem.* **2013**, *85*, 11163–11173. [[CrossRef](#)] [[PubMed](#)]
95. Snijder, J.; van de Waterbeemd, M.; Damoc, E.; Denisov, E.; Grinfeld, D.; Bennett, A.; Agbandje-McKenna, M.; Makarov, A.; Heck, A.J. Defining the stoichiometry and cargo load of viral and bacterial nanoparticles by Orbitrap mass spectrometry. *J. Am. Chem. Soc.* **2014**, *136*, 295–299. [[CrossRef](#)] [[PubMed](#)]
96. Nakabayashi, R.; Sawada, Y.; Yamada, Y.; Suzuki, M.; Hirai, M.Y.; Sakurai, T.; Saito, K. Combination of liquid chromatography-Fourier transform ion cyclotron resonance-mass spectrometry with ¹³C-labeling for chemical assignment of sulfur-containing metabolites in onion bulbs. *Anal. Chem.* **2013**, *85*, 1310–1315. [[CrossRef](#)] [[PubMed](#)]



© 2015 by the authors; licensee MDPI, Basel, Switzerland. This article is an open access article distributed under the terms and conditions of the Creative Commons by Attribution (CC-BY) license (<http://creativecommons.org/licenses/by/4.0/>).